1990

Performance Evaluation of Rotary Compressor with Special Attention to the Accuracy of P-V Diagram

K. C. Moun
Goldstar Co.

Y. Tae-Hwan
Goldstar Co.

K. Tae-Jong
Goldstar Co.

L. Sung-Bae
Goldstar Co.

E. Yoon-Seob
Goldstar Co.

See next page for additional authors

Authors
K. C. Moun, Y. Tae-Hwan, K. Tae-Jong, L. Sung-Bae, E. Yoon-Seob, and S. Chun-Mo

PERFORMANCE EVALUATION OF ROTARY-COMPRESSOR WITH SPECIAL ATTENTION TO THE ACCURACY OF P-V DIAGRAM

MOUN KYU-CHAN, YOUN TAE-HWAN, KIM TAE-JONG, LEE SUNG-BAE, EOM YOON-SEOB, SUNG CHUN-MO.
GOLDSTAR CO., LTD. CHANGWON PLANT. 391-2 GAEUMJEONG-DONG
CHANGWON CITY, GYEONG NAM, KOREA.

ABSTRACT

For the compressor compression performance evaluation of the rolling piston type refrigeration compressor (horizontally installed type), which are used in household refrigerator, and freezer, we have obtained pressure-volume diagram experimentally.
By the differences in chamber shell thickness and discharge cavity volume within chamber shell that are resulted from the installation of pressure transducers and gap sensors, there are large heat transfer losses in measured P-V diagram which are different in P-V diagram from real compressor, and we have confirmed the relationship of the pressure pulsations and valve behavior by measuring valve behavior to compression ratio(Ps/Pd).

INTRODUCTION

Generally in the refrigeration and air-conditioning industry, some of the most common terms used to indicate the compressor performance are coefficient of performance(COP), energy efficiency ratio(EER), these terms are convenient for the purpose of rating in the compressors, post-production testing and consumer information, but it is not helpful to the objective evaluation of any particular compressor design either at the design stage or for a comparative study of various designs.
That is, there are not a detailed evaluation in energy and mass flow losses which have an effect on COP and EER, so we can't perform model comparision and evaluation.
In this paper, after we have measured P-V diagram in connection with compressor compression process, and have computed the energy losses in operating condition, we are going to evaluate compressor compression performance.

P-V DIAGRAM AND LOSS CALCULATION.

For the analyzing method of the detailed distribution and rates of losses in a rotary compressor, there are loss calculation by a P-V diagram measurement.
FIG.1 is a typical P-V diagram of the rotary compressor and Fig.2 represents various losses.

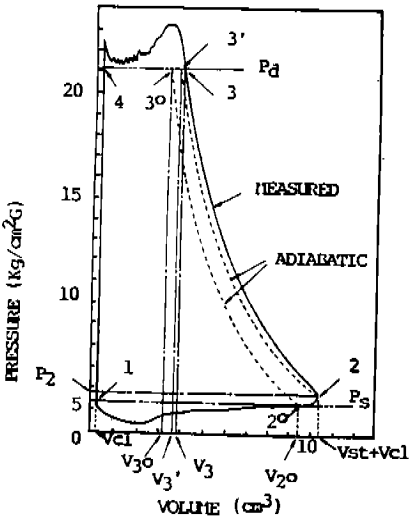

FIG.1 TYPICAL P-V DIAGRAM

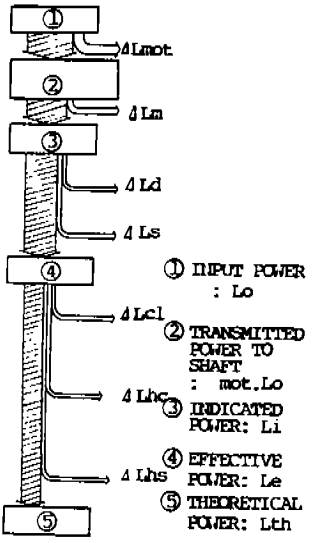

FIG.2 FLOW OF POWER IN THE COMPRESSOR

Definitions of the work rates and losses are as follows

(1) Li : INDICATED POWER (WORK WHICH IS ACTUALLY GIVEN TO GAS IN THE CYLINDER : AREA S_{1234})

(2) Ld : DISCHARGE PASSAGE LOSS (OVER-SHOOTING LOSS : $S_{3'4}$)

(3) Ls : SUCTION PASSAGE LOSS (UNDER-SHOOTING LOSS : S_{12^o})

(4) Le : EFFECTIVE POWER (COMPRESSION WORK OF GAS FROM LOW PRESSURE SIDE TO HIGH PRESSURE SIDE(Ps ⟶ Pd))

(5) Lcl : CLEARANCE VOLUME LOSS (REEXPANSION LOSS)

(6) Lhc : HEAT LOSS DURING COMPRESSION PROCESS ($S_{23'3}$)

(7) Lhs : HEAT LOSS DURING SUCTION PROCESS

Lcl + Lhs : LOSS OCCURRING DURING SUCTION PROCESS UP TO STARTING OF COMPRESSION PROCESS ($S_{2^o3^o3'2}$)

(8) Lth : THEORETICAL POWER (ADIABATIC WORK, $S_{12^o3^o4}$)

EXPERIMENTAL SETUP AND PROCEDURES

Test compressor : Fig.3 is the cross-section of the real and test compressor. In the test compressor, which is used for measuring dynamic pressures within cylinder, valve behavior, instantaneous angular positions of the revolution and TDC-MARKER, 3 piezoelectric pressure transducers and 3 gap sensors are installed at their positions. For the installation cavity of the these sensors, we redesigned chamber shell with a flange surface to bolt screwing, so chamber shell is thicker than the real chamber shell.

Pressure measurements : The calibration of the pressure transducers completed before installing in test compressor, it is confirmed by drawing up the calibration chart which represents the relationship between the pressure in pressure vessel and the output voltage passed by the charge amplifier.

In order to measure the dynamic pressures within cylinder, pressure transducers are installed as Fig.4. In the design of the pressure transducer adapter system, we have used plane wave acoustic theory and calculated resonance frequency of the adapter system by the HELMHOLTZ EQN., ORGAN PIPE EQN., ELECTRICAL ANALOGY METHOD. Calculation results are in Table 1.

Gap measurements : from the geometrical relations of the cylinder, roller and vane (Fig.7), the eqn. of the cylinder volume with respect to angular positions is derived as follows

$$V(\theta)=hRc^2/2\ [(1-a^2)\theta-(1-a^2)\sin 2\theta/2-a^2\sin^{-1}((1/a-1)\sin\theta)-a(1-a)\sin\theta$$
$$\sqrt{1-(1/a-1)^2\sin^2\theta}-(t'h/2)Rc(1-(1-a)\cos\theta-\sqrt{(1-a)^2\cos^2\theta+2a-1})]$$

V(θ) : ACTUAL VOLUME CORRESPONDING TO POSITION θ

Rc : CYLINDER RADIUS, R : RADIUS VECTOR, Rr : ROLLER RADIUS

h : CYLINDER or BLADE HEIGHT, a : RADIUS RATIO(Rr/Rc) : DIMENSIONLESS

θ : ANGULAR POSITION OF ROTOR, Ø : ARBITRARY ANGLE, t : BLADE THICKNESS

Be : BLADE EXTENSION, e : ECCENTRICITY

Measurements of the instantaneous angular position consists of 2 gap sensors and timing gear, one of 2 gap sensors is installed vertically to timing gear to sense instantaneous angular position (Fig.6)
Gap measurements are valve behavior, TDC-MARKER, instantaneous angular position, and gap sensors are fixed closely to measuring objects so that the signal is generated accurately. Flange surface which is placed at chamber shell is sealed by "O-RING", and by using BNC-CONNECTOR, signal cables are connected through chamber shell, and BNC-CONNECTOR is fixed to chamber shell by brazing.

SIGNAL PROCESSING

Fig.9 is a schematic diagram of the data acquistion system.
External trigger signal which is TDC-MARKER signal of the ploximitor probe is passed by TTL DEVICE and it is connected to digital input channel within A/D converter board, in another way, when it is connected to analog input channel, it can be used to software trigger. Input signals of pressure and valve behavior are connected to A/D converter via analog multiplexer and converted to digital datas, which are memorized at RAM part within PERSONAL COMPUTER and transferred to floppy diskette or hard disc of P/C.
In the same manner, instead of the A/D converter, we can use commercial digital oscilloscope, then it is more accurate and powerful in signal processing.

RESULTS AND DISCUSSION

In timing gear signal of Fig.10, the revolution speed of crankshaft is nearly constant within the limits of sampling interval, so TSM(TIME SAMPLING METHOD) can be used. In the same manner, we can measure crankshaft revolution speed accurately in a operating condition. From Fig.11,12,13, valve opening time

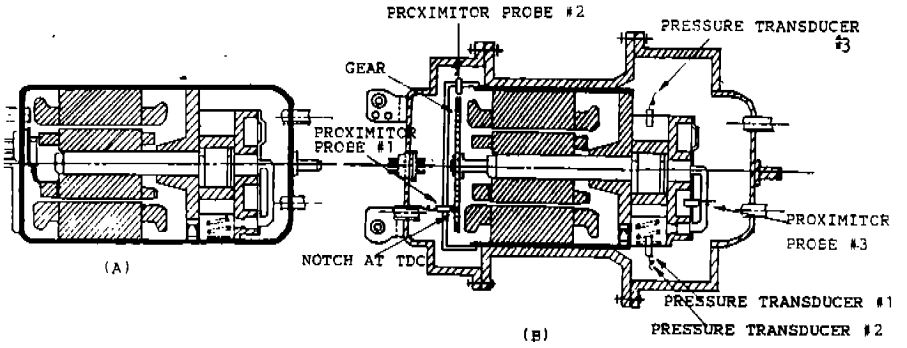

Fig.3 CROSS-SECTION OF REAL COMPRESSOR(A) AND TEST COMPRESSOR.(B)

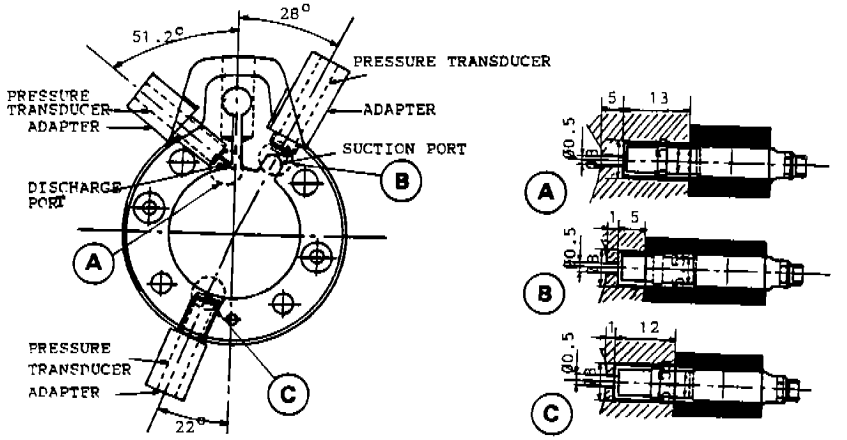

Fig.4 DESIGN OF PRESSURE TRANSDUCER ADAPTER

TABLE 1 RESONANCE FREQUENCY ANALYSIS.

	MODELLING & EQN.	RESULT
SET I (B)	1.HELMHOLTZ EQN. $(0 \leq R \leq 100)$ $f_1 = \frac{c}{2\pi l_1'} \times \frac{1}{\sqrt{R+0.3905}}$	$l_1' = l_1 + \pi r/4 = 1.196$mm $R = V_1/V_2 = 10.3$, $C = 150$m/s $f_1 = 6104$Hz $f_2 = 31350$Hz
SET II (C)	2.ORGAN PIPE EQN. $(R \fallingdotseq 0)$ $f_2 = \frac{(2N+1)}{4} \times \frac{C}{l_2'} = (n=0,1,2\ldots)$	$c = 155$m/s $f_1 = 6308$Hz $f_2 = 32400$Hz
SET III (A)	3.$l_2/r > 8$, ELECTRICAL ANALOGY $f = \sqrt{\frac{3}{16\pi}} \frac{r.c}{\sqrt{l_2 \times V_1}}$	$C = 168$m/s, $V = 2419$mm $f_1 = 2949$Hz $f_2 = 7700$Hz $f_3 = 2810$Hz

is determined, by this time, we can convert voltage level of discharge pressure signal into gage pressure level.
By measuring valve behavior accurately, reexpansion of the refrigerant gas in clearance volume is confirmed. It is ideal valve behavior when pressure within cylinder reaches discharge pressure, valve opens swiftly and closes without fluttering from Fig.14,15,16, valve behaves in accord to compression ratio, as ratio valve is higher, fluttering phenomena become seriously.
Ideal valve behavior is virtually impossible to satisfy for compressors that have to run at a variety of operating conditions.
So acceptable valve behavior in the vicinity of the so called design condition, which is usually the operating condition at which the compressor statistically most often operates can be designed.
From Fig.17,18,19, as pressure level of the discharge gas is higher than usual, compression process is far from adiabatic process, so heat loss becomes large amounts.
From Fig.20, we represent all the measured data.
From Fig.21, in the classification and rates of losses of the P-V diagram, heat loss in compression process of the test compressor is larger than real compressor by the chamber shell thickness and differences in discharge cavity volume.

CONCLUSIONS

For the test compressor setup and signal processing procedures, P-V diagram is measured which classify and calculates overshooting and undershooting loss, leakage and heat transfer loss and clearance volume and reexpansion loss. And it is more efficient to use commercial digital oscilloscope by the high speed revolution of the rotary compressor.
In measured P-V diagram, it is different in heat transfer through chamber shell from real compressor.
So performance analysis through P-V diagram measurements is more effective in using MODEL comparision, evaluation.

REFERENCES

1. H. WAKABAYASHI ET AL : "Analysis of performance in a rotary compressor" PCTC 1982, PURDUE UNIVERSITY.
2. Pandeya, P & Soedel, "Rolling piston type rotary compressors with special attention to friction & leakage" PCTC 1978, PURDUE UNIVERSITY
3. E. SAKURAI & HAMILTON, J, F "Measurement of operating conditions of rolling piston type rotary compressors" PCTC 1982, PURDUE UNIVERSITY.

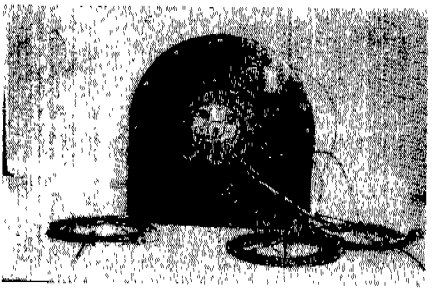

Fig.5 PRESSURE TRANSDUCER MOUNTED

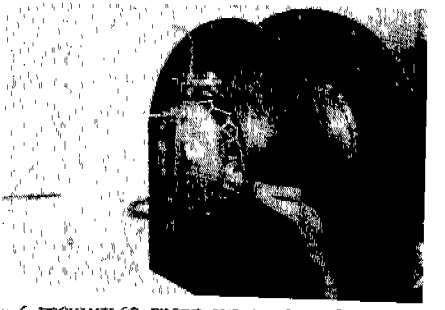

Fig.6 PROXIMITOR PROBE AND A GEAR MOUNTED

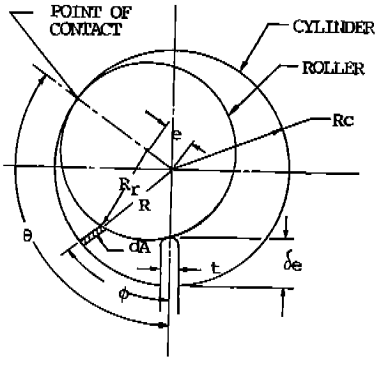

Fig.7. VOLUME-ANGLE RELATIONSHIP

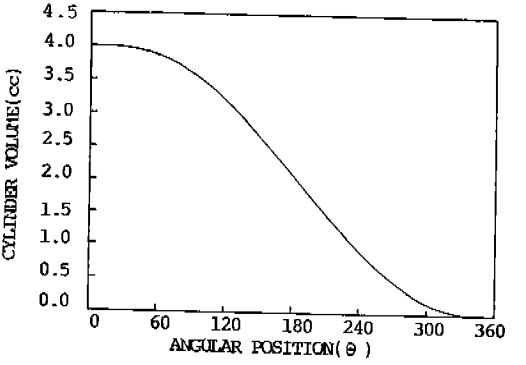

Fig.8. V-θ DIAGRAM

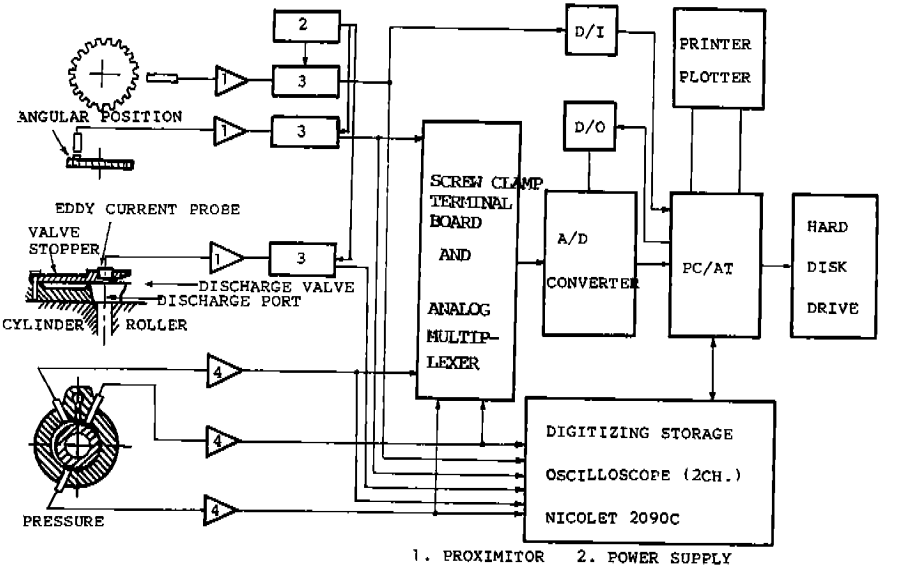

1. PROXIMITOR 2. POWER SUPPLY
3 PROXIMITOR TRANSDUCER 4. CHARGE AMP.

Fig.9. MEASUREMENT SYSTEM

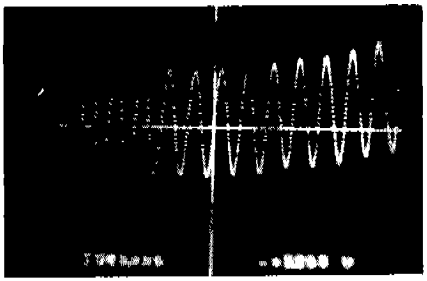

Fig.10 WAVE FORM OF TIMING GEAR

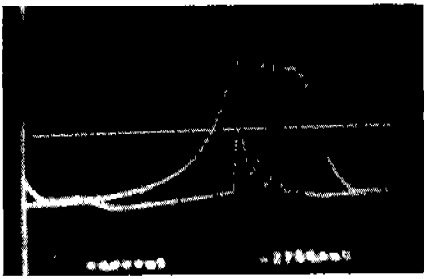

Fig.11 DISCHARGE PRESSURE & VALVE BEHAVIOR

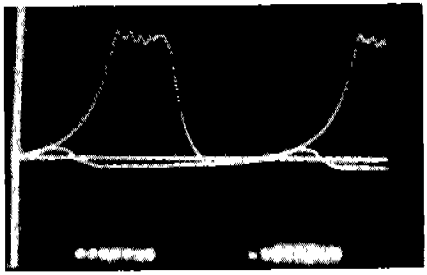

Fig.12 DISCHARGE PRESSURE FLUCTUATION & REFERENCE PRESSURE

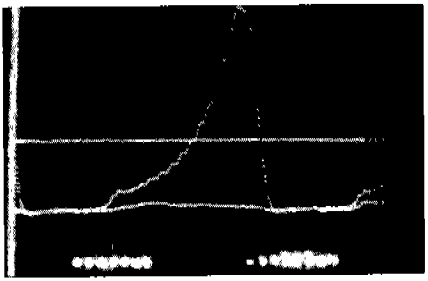

Fig.13 SUCTION PRESSURE FLUCTUATION & REFERENCE PRESSURE

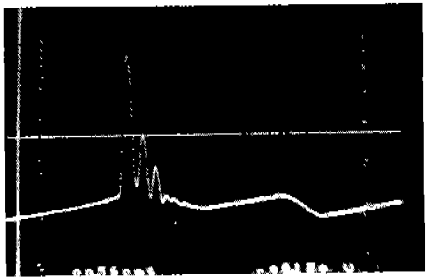

Fig.14 VALVE BEHAVIOR(I)
(Ps/Pd=0.01/5)

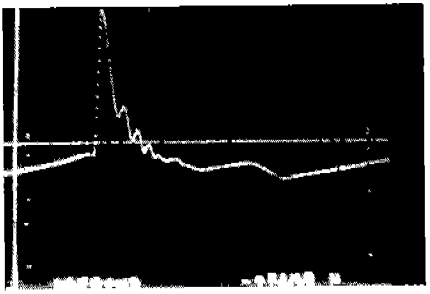

Fig.15 VALVE BEHAVIOR (II)
(Ps/Pd=0.1/10.3)

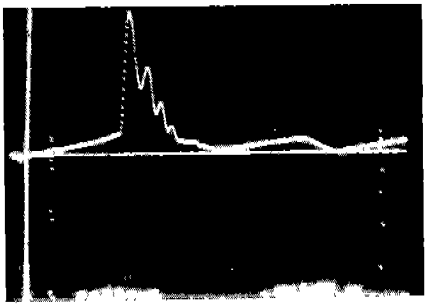

Fig.16 VALVE BEHAVIOR (III)
(Ps/Pd=0.6/14)

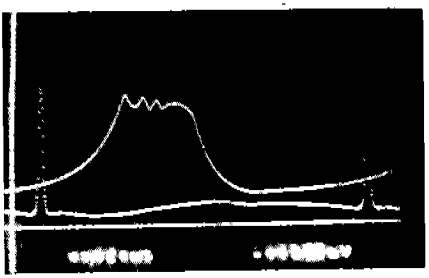

Fig.17 DISCHARGE PRESSURE FLUCTUATION (I)
(Ps/Pd=0.01/5)

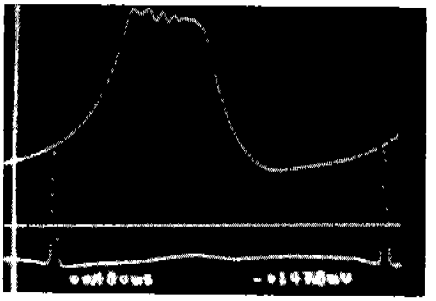

Fig.18 DISCHARGE PRESSURE FLUCTUATION(II) (Ps/Pd = 0.1/10.3)

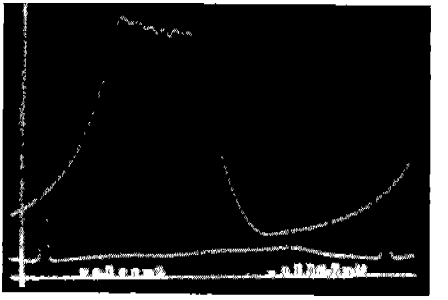

Fig.19 DISCHARGE PRESSURE FLUCTUATION(III) (Ps/Pd = 0.6/14)

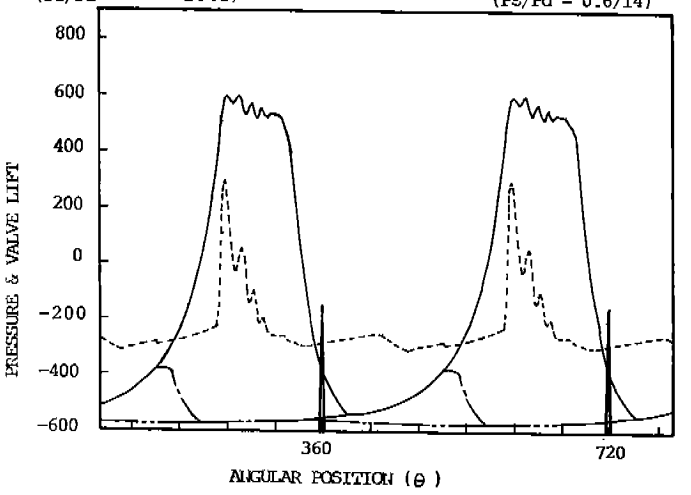

Fig.20 MEASURED PRESSURE VARIATION, VALVE BEHAVIOR & TDC-MARKER (Ps/Pd = 0.1/10.3 Kgf/cm^2.G)

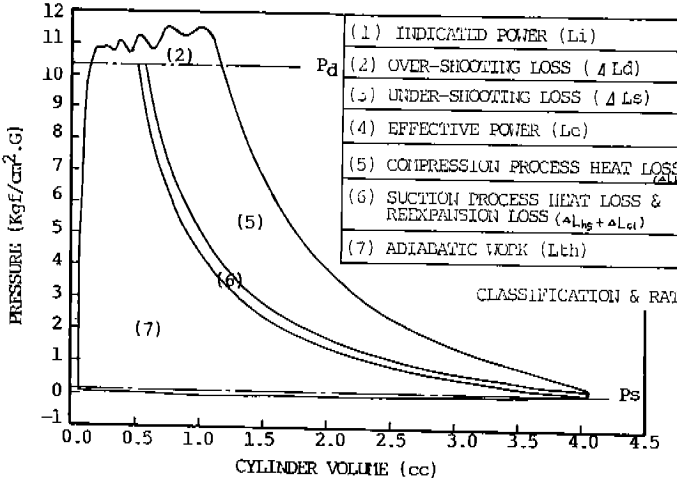

(1) INDICATED POWER (Li)	107.46W (100%)
(2) OVER-SHOOTING LOSS (Δ Ld)	4.64 (4.32)
(3) UNDER-SHOOTING LOSS (Δ Ls)	2.01 (1.87)
(4) EFFECTIVE POWER (Lc)	100.81W(93.81%)
(5) COMPRESSION PROCESS HEAT LOSS (ΔL_{hc})	41.01 (38.16)
(6) SUCTION PROCESS HEAT LOSS & REEXPANSION LOSS ($\Delta L_{hs} + \Delta L_{ex}$)	6.64 (6.18)
(7) ADIABATIC WORK (Lth)	53.16W (49.47%)

CLASSIFICATION & RATES OF LOSSES.

Fig.21. MEASURED P-V DIAGRAM (Ps/Pd=0.1/10.3 Kgf/cm^2.G)